Unexpected Intermediate State Photoinduced in the Metal-Insulator Transition of Submicrometer Phase-Separated Manganites

Hanxuan Lin, Hao Liu, Lingfang Lin, Shuai Dong, Hongyan Chen, Yu Bai, Tian Miao, Yang Yu, Weichao Yu, Jing Tang, Yinyan Zhu, Yunfang Kou, Jiebin Niu, Zhaohua Cheng, Jiang Xiao, Wenbin Wang, Elbio Dagotto, Lifeng Yin, and Jian Shen

Phys. Rev. Lett. **120**, 267202 — Published 28 June 2018

DOI: 10.1103/PhysRevLett.120.267202

Unexpected Intermediate State Photoinduced in the Metal-Insulator Transition of Submicrometer Phase Separated Manganites

Hanxuan Lin[1], Hao Liu[1], Lingfang Lin[2], Shuai Dong[2], Hongyan Chen[1], Yu Bai[1], Tian Miao[1], Yang Yu[1], Weichao Yu[1], Jin Tang[3], Yinyan Zhu[1], Yunfang Kou[1], Jiebin Niu[1], Zhaohua Cheng[3], Jiang Xiao[1,5,6], Wenbin Wan[1,4], Elbio Dagotto[7,8*], Lifeng Yin[1,6*], and Jian Shen[1,6*]

[1]*State Key Laboratory of Surface Physics and Department of Physics, Fudan University, Shanghai 200433, China*

[2]*School of Physics, Southeast University, Nanjing 211189, China*

[3]*Beijing National Laboratory for Condensed Matter Physics, Chinese Academy of Sciences, Beijing 100190, China*

[4]*Advanced Materials Laboratory, Fudan University, Shanghai 200433, China*

[5]*Institute for Nanoelectronics Devices and Quantum Computing, Fudan University, Shanghai 200433, China*

[6]*Collaborative Innovation Center of Advanced Microstructures, Nanjing 210093, China*

[7]*Department of Physics and Astronomy,University of Tennessee, Knoxville, TN 37966, USA and*

[8]*Materials Science and Technology Division, Oak Ridge National Laboratory,Oak Ridge, TN 37831, USA*

(Dated: May 30, 2018)

At ultrafast time scales, the initial and final states of a first-order metal-insulator transition often coexist forming clusters of the two phases. Here, we report an unexpected third long-lived intermediate state emerging at the photoinduced first-order metal-insulator transition of $La_{0.325}Pr_{0.3}Ca_{0.375}MnO_3$, known to display submicrometer length-scale phase separation. Using magnetic force microscopy and time-dependent magneto-optical Kerr effect, we determined that the third state is a nanoscale mixture of the competing ferromagnetic metallic and charge-ordered insulating phases, with its own physical properties. This discovery bridges the two different families of colossal magnetoresistant manganites known experimentally and shows for the first time that the associated states predicted by theory can coexist in a single sample.

PACS numbers: 71.27.+a, 71.30.+h, 73.50.Pz, 42.82.Cr, 07.79.Pk

Introduction. Electronic phase separation is common in first-order phase transitions because the two competing phases have similar free energies. In first-order metal-insulator transitions [1–4], the coexistence of the metallic and insulating phases was observed in various strongly correlated systems [5–8]. However, no additional stable intermediate state has been experimentally reported, at least in strongly correlated magnetic systems, albeit ultrafast transient phases were occasionally identified [9–11]. In strongly correlated materials, first-order metal-insulator transitions are not only driven by temperature, but by other external stimuli [9] such as electric [10] and magnetic [1] fields, pressure [11], and light [12].

Photoinduced rapid transient effects are common in correlated systems [12, 13], but persistent photoinduced metal-insulator transitions have only been reported in a few cases [14, 15], such as the manganites [15–17], the materials with the colossal magnetoresistance (CMR) effect. Previous efforts on manganite's photoinduced phase transitions using optical and magnetic microscopy identified the ferromagnetic metallic (FMM) and charge-ordered insulating (COI) regions [18–21]. However, due to resolution effects, limited information was gathered on the spatial distribution of electronic domains with submicron or smaller length scales. Transient states in the ultrafast timescale can be revealed with pump-and-probe techniques [9, 22–24], but the analysis of the evolution and dynamics of individual electronic domains is lacking.

In this work, we show that in manganites a stable intermediate state appears and coexists with the FMM and COI phases [25] during photoinduced phase transitions. Although ultrafast transient phases were identified before [26–28], stable intermediate states are rare [6–8, 28], and the nature and physical origin of such intermediate states is basically unknown. In our present effort, the stable intermediate state was directly visualized by using a variable temperature magnetic force microscope (MFM), coupled with optical fiber for photoexcitation (Fig. 1a). With the help of time-dependent magneto-optical Kerr effect measurements (MOKE), we conclude that the nature of the intermediate state is a nanoscale mixture of the FMM and COI phases. Despite its mixed-phase nature, this is regarded as an intermediate independent state because it displays its own characteristic length scale and properties and, moreover, we argue it resembles the high temperature "CMR" state with correlated polarons widely studied before in other manganites.

Results. Thin films of $La_{0.325}Pr_{0.3}Ca_{0.375}MnO_3$ (LPCMO) in epitaxial form were chosen as the model system. LPCMO is well-known for its large length scale (submicrometer on average) electronic phase separation [29–34]. 40 nm LPCMO films were grown on (001) ori-

*To whom correspondence should be addressed

ented $LaAlO_3$ (LAO) substrates. The insulator-to-metal transition (IMT) and the metal-to-insulator transition temperatures (MIT) of LPCMO thin films were determined to be 123 K and 185 K (Fig. S1 [35]). The photoexcitation of the sample was achieved using nanosecond pulsed laser (532 nm, 1.3 ns, 2 kHz) during the warming process from 10 K [42].

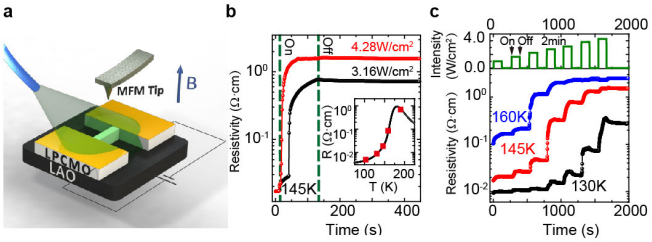

FIG. 1: (color online) (a) Sketch of the MFM set-up and geometry of the device for transport measurements. (b) Two resistivity measurements with different light intensities at 145 K, separated by a thermal cycle to room temperature (the photo-induced changes in ρ are persistent and irreversible, unless a thermal cycle is performed). Green dash lines denote the switch on-off times. Inset: ρ vs temperature upon warming, with red dots denoting the temperatures where experiments were conducted. (c) Light-intensity dependent ρ measured within a single thermal cycle at 130 K, 145 K, and 160 K. The lighting process is in the upper panel.

Global transport measurements indicate that ρ changes sensitively depend on light intensity. Figure 1b shows the ρ response after light exposure. The black and red curves were recorded at 145 K when the sample was exposed to light for two minutes with light intensities, respectively, 3.16 and 4.28 W cm^{-2} (average light intensity of the pulsed laser) [43]. In both cases, light increased ρ by nearly two orders of magnitude. The higher the light intensity is, the larger ρ becomes. ρ stays nearly unmodified after light is switched off. Such persistence implies that the light-induced transport changes cannot be attributed to a temperature increase caused by a trivial laser heating effect (Sec. III [35]).

To study the photoinduced MIT microscopically, MFM is used (Sec. Method [35]) to capture the evolution of the FMM and COI domains with increasing light intensities as follows: (1) After a full thermal cycle, a chosen temperature is reached upon warming; (2) At this fixed temperature, the sample is opened to two-minute light exposure with a fixed light intensity and MFM images are subsequently acquired. Step 2 is then repeated for increasingly higher light intensities. This procedure avoids different thermal cycles to reset domain patterns (Fig. S3 [35]), allowing to follow the evolution of electronic domains during the transition (Sec. I [35]). Five chosen temperatures are indicated by the red dots in the warming ρ vs T curve in Fig. 1b (inset). To correlate the MFM images with the global transport measurements for further analysis, the changes in ρ measured by following this procedure at 130 K, 145 K, and 160 K are in Fig. 1c [44].

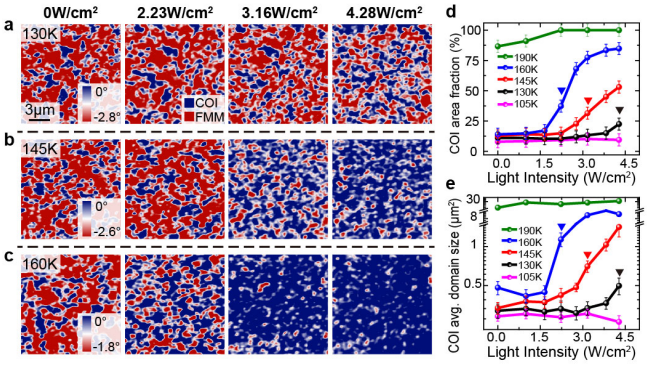

FIG. 2: (color online) (a)-(c) $15\mu m \times 15\mu m$ MFM images acquired at 130 K, 145 K, and 160 K. The scanning area is fixed at each temperature and its displacement between different temperatures is within 1 μm (for topography see Fig. S2 [35]). Left to right, the light intensity increases from 0 to 4.28 W cm^{-2}. Blue and red regions are the COI and FMM phases, respectively. The MFM signal (phase shift) ranges are the same for each temperature but tuned to a proper level at different temperatures for better presentation (2.8, 2.6, and 1.8 degrees for 130, 145, and 160 K, respectively). Note that the MFM signal is negative (positive) for the magnetic (nonmagnetic) phase right above the LPCMO film (Sec. Method [35]). (d)-(e) Statistics from the MFM images vs light intensity at different temperatures: both the area fraction of COI state (d) and average size of COI domains (e) increase rapidly at some critical light intensities (arrows). Error bars are standard (Sec. II [35]).

The MFM images with increasing light intensities at 130 K, 145 K, and 160 K (Figs. 2 a-c) are consistent with the transport data (see Fig. S2 [35] for all five temperatures). All MFM images were acquired under a small 500 Oe perpendicular field [45] (Fig. S3 [35]). The MFM signal (phase shift of the tip) taken right above the LPCMO film is negative (positive) for the magnetic (nonmagnetic) phase (Sec. Method [35]). We observed that at a fixed temperature both the area fraction of the COI phases (Fig. 2d) and the average size of the COI domains (Fig. 2e) increase rapidly at particular light intensities (arrows in Figs. 2d and e), which shift towards lower values upon increasing temperature.

Remarkably, besides the usual LPCMO coexistence of FMM and COI phases, we found the unexpected presence of a photo-induced *third state* (white) which is stable with time. Note that as "third state" we refer specifically to the white islands extending away from the FMM domains, namely we exclude the white edges surrounding the FMM domains which may be induced by stray fields spreading out of the FMM domains and are observed in the MFM images before light illumination as well. Our results are better presented via magnified MFM images with marked line profiles, where three distinct MFM sig-

nal levels show up, corresponding to the FMM and COI phases, as well as the novel third state (Fig. 3a). The histograms of the MFM signal obtained from the MFM images clearly evolve from a bimodal distribution (the FMM and COI phase) to a trimodal distribution (the FMM, COI, and third state) with increasing light intensity at 130 K, 145 K, and 160 K (Fig. 3b and Fig. S4 [35]). Without photo-excitation, there is no third peak appearing by a regular temperature increase procedure, which strongly rules out trivial heating effects as the origin of the stable third state (Sec. III [35]). The area fraction of each state can be obtained from the histograms (the weight of corresponding peaks) and plotted vs light intensity (Fig. 3c). We observed that the third state first increases and then decreases its fraction with increasing light intensity at 160 K, implying that the FMM phase transits to the COI phase with the third state as intermediary. In this sense, the exotic third state is a photoinduced intermediate state mediating the transition. To better demonstrate the mediatory role of this state, a movie was filmed by combining 32 frames of MFM images acquired at the same position at 145 K (Movie S1 [35]). Unambiguously, the intermediate state begins to appear at a certain light intensity, then expands to a maximum area fraction, and finally transits to the insulating phase.

In terms of magnetic properties of the intermediate state, its weak MFM signal (Figs. 3a and b) indicates a weak perpendicular components of the magnetization (Sec. Method [35]). This may originate from various magnetic structures such as a ferromagnetic phase with enhanced in-plane magnetic anisotropy, a low-spin ferromagnetic regime, a canted antiferromagnetic state, or a nanoscale mixture of FMM and COI phases. Among them only the nanoscale mixture contains the nanoscale ferromagnetic domains which will exhibit a superparamagnetic behavior [46] and result in the time-decay of the remnant magnetization at temperatures not far below the blocking temperature [47, 48].

Figure 4 shows time-dependent magneto-optic Kerr effect (MOKE) measurements before and after photoexcitation (Sec. Method [35]). In the thin-film limit, the measured Kerr intensity is proportional to the total net moment of the magnetic thin films [47, 49]. From the magnetic loops swept between ±650 Oe, M_{650} and M_R are defined as the Kerr intensity at 650 Oe and the remnant Kerr intensity after the magnetic field is back to 0 Oe, respectively (insets in Figs. 4a-b). At 145 K before the photoexcitation, a time-dependent MOKE measurement was performed after demagnetization. The Kerr intensity rises from zero to M_{650} within half a second after a 650 Oe magnetic field is applied. After the magnetic field is switched off, the Kerr intensity drops to M_R, also within half a second, and remains constant afterwards (Fig. 4a). Such stable M_R is expected because the submicron FMM domains are large enough to exhibit ferromagnetic behavior. However, as the same measurement was conducted to

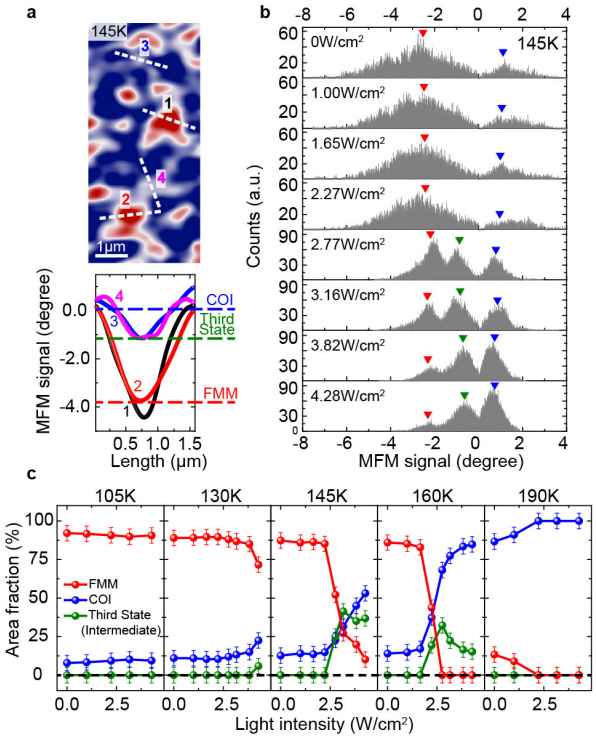

FIG. 3: (color online) (a) Line profiles (lower panel) obtained from the MFM images at 145 K with 3.16 W cm^{-2} light intensity along the lines indicated in the upper panel, showing the coexistence of three states: COI (blue), third state (white), and FMM (red). Line profiles (1.5 μm long) are cut across two FMM domains (1 and 2) and two third state domains (3 and 4). The COI phase is shown at the two ends of every line profile (1 to 4). The MFM signal range is the same as in Fig. 2b. (b) Histograms of the MFM signal obtained from the MFM images at 145 K, evolving from a bimodal to a trimodal distribution with increasing light intensity. The emerging third peak corresponds to the third state (green triangles), while the FMM and COI peaks are the red and blue triangles, respectively. The positions of the triangles are determined by multi-peak Gaussian fitting. (c) Area fraction of all three states: FMM, third, and COI states vs light intensity for five temperatures, illustrating the mediatory role of the third state.

the LPCMO film after two-minute light exposure (4.68 W cm^{-2}, Fig. 4b), the Kerr intensity is no longer stable and clearly decays with time after reaching the corresponding M_R, compatible with having an appreciable amount of nanoscale FMM domains created by light [47, 48]. The typical domain diameter is determined to be ∼15 nm by fitting the decay curve (Sec. Method [35]). Because the pronounced existence of nanoscale FMM domains coincides with the large population of the intermediate state, this strongly suggests that the intermediate state is a FMM-COI nanoscale mixture.

Discussion. This mixing of nanoscopic structures cannot be considered as a mere special case of the well-know submicrometer phase separated FMM-COI state

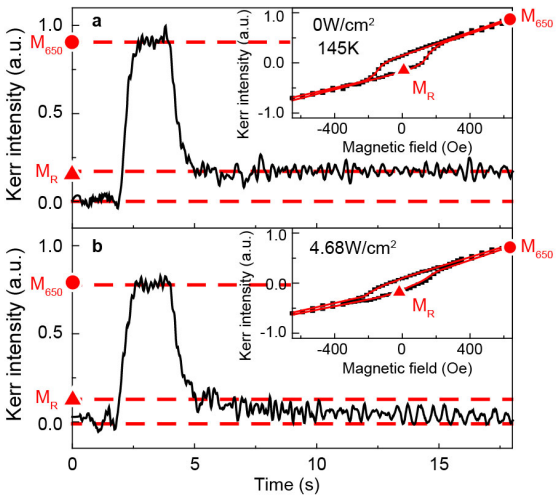

FIG. 4: (color online) MOKE measurements before (a) and after (b) photoexcitation at 145 K. Time resolution is 30 ms and the light intensity is 4.68 W cm^{-2}, where the intermediate state is prominent. Both in (a) and (b), dashed lines are the Kerr intensity levels for zero (demagnetized state), for M_{650}, and for M_R (M_{650} and M_R are the Kerr intensities at 650 and 0 Oe, respectively, consistent with those determined from the magnetic hysteresis loops in the insets of (a) and (b)). After switching off the external magnetic field, the Kerr intensity falls rapidly from M_{650} to M_R. Having reached M_R, the Kerr intensity is stable before photoexcitation (a) and clearly decays increasing time after photoexcitation (b). The latter is a typical superparamagnetic behavior displayed by nanoscale FMM domains, indicating that the intermediate state is a nanoscale mixture of FMM and COI phases. Kerr intensity was normalized to one for better presentation.

of LPCMO, otherwise there should not be a third independent peak in the histogram after photo-excitation (Fig. 3b). Its coexistence with the submicron FMM and COI phases leads to a phenomenon not reported before to our knowledge: photoexcitation generates *two dramatically different electronic phase separation length scales* (nanometer and submicrometer).

Regarding the origin of the third state, since it is not observed upon static heating, we believe this stable intermediate state is induced by photoexcitation, but it could be possible that a *transient* nanoscale mixing state can be created by static heating which can not be captured by slow MFM measurements. We also believe its formation could be related to the superfast temperature change induced by the intense pulsed laser (up to 4.00 MW cm^{-2} per pulse), which may result in electronic phase separation with a much smaller length scale. These nanoscopic domains will freeze after the temperature rapidly drops back, forming the observed intermediate state, which is verified by a numerical simulation based on the random-field Ising model (RFIM) [53–55]. Nanoscale mixture of the FMM and COI phases does form in the simulation giving results similar to experiments (Sec. V and Fig. S5 [35])

The scientific significance of the third state lies in the theoretical predictions [56] that unified in a single framework the phenomenological behavior of the two different families of CMR manganites observed experimentally. Those early predictions were based on transport data for $(Nd_{1-y}Sm_y)_{1/2}Sr_{1/2}MnO_3$ [57] that displays two different CMR's varying temperature. The submicron length-scale phase separation of LPCMO fits into the so-called "CMR1" (or low-temperature CMR) behavior discussed in [56] (Figs. 5a and b), while interpenetrating nanometer length-scale FMM and COI domains is compatible with the "CMR2" (or high-temperature CMR) behavior [56] (Figs. 5a and c), typical of canonical CMR manganites such as $La_{1-x}Ca_xMnO_3$ (LCMO). The primary merit of our observation is that for the first time the states related with both types of CMR's are displayed in real-space "snapshots" for the same sample, thus unifying these two families of manganites. Our results lead to the intriguing conclusion that the CMR2 state with nanometer-scale phase coexistence of LCMO is located only at slightly higher energy than the thermodynamically stable states of LPCMO, and it can be induced by light applied to LPCMO that in equilibrium only is characterized by CMR1 behavior.

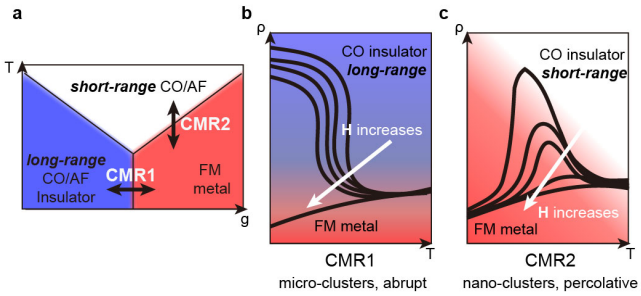

FIG. 5: (color online) (a) Theoretically predicted generic phase diagram when FMM and COI states compete [56]. The expected micrometer-scale CMR1 and nanometer-scale CMR2 phenomena, see text, are shown. g represents a generic variable needed to transfer the system from one phase to the other [56], such as the tolerance factor. (b) Magnetic field H evolution of ρ vs temperature for CMR1, from the COI to the FMM, involving an abrupt first-order transition and concomitant micrometer-scale phase separation. (c) Same as (b) but for CMR2, involving a percolative process and nanometer-scale phase separation.

Note that our observation is *not* limited to manganites. A long-lived metastable state involving ordered polarons has been reported before in a layered dichalcogenide $1T-TaS_2$ [58], which shares qualitative similarities with our work. In particular, in the field of manganites states that compete with the FMM state are often described as made of correlated polarons, imagined as a periodic distribution of polarons forming patterns rather than a random gas of polarons [59]. And the physics of CMR is also not limited just to manganites, but similar

ideas are applicable to several transition metal oxides and other compounds, such as Ru-, Cu-, and Co-oxides, with inhomogeneous dominant states [60], particularly when several degrees of freedom are simultaneously active.

In summary, we have visualized a previously unidentified intermediate state in LPCMO manganites during the photoinduced MIT. Once generated, the intermediate state is long-lived and distinctly different from previously reported photoinduced transient states at ultrafast timescales. We believe this intermediate state is a mixture of FMM and COI nanoscale domains. Although more detailed understanding about the intermediate state should be gathered in future experiments, the observation of the photoinduced intermediate state not only bridges the two types of CMR transitions in manganites, but also illustrates a way to create two completely different characteristic lengths of phase separation in first order metal-insulator transitions, which may be applicable to first-order metal-insulator transitions in other condensed matter systems as well.

Acknowledgments. Work supported by the National Key Research Program of China (2016YFA0300702), National Basic Research Program of China (973 Program) under grants No. 2013CB932901 and 2014CB921104, National Natural Science Foundation of China (11274071, 11504053, 11674055, 11474065), and the Shanghai Municipal Natural Science Foundation (14JC1400500, 18JC1411400, 18ZR1403200). E.D. was supported the US Department of Energy, Office of Basic Energy Sciences, Materials Sciences and Engineering Division.

[1] S. Jin, T. H. Tiefel, M. Mccormack, R. A. Fastnacht, R. Ramesh, and L. Chen, Science **264**, 413 (1994).
[2] M. M. Qazilbash, M. Brehm, Byunggyu Chae, P. C. Ho, G. O. Andreev, Bongjun Kim, Sun Jin Yun, A. V. Balatsky, M. B. Maple, Fritz Keilmann, Hyuntak Kim, and D. N. Basov, Science **318**, 1750 (2007).
[3] B. Radisavljevic and A. Kis, Nature Mater. **12**, 815 (2013).
[4] L. Nagarajan, Roger A De Souza, D. Samuelis, I. Valov, A. Borger, J. Janek, K. D. Becker, P. C. Schmidt, and M. Martin, Nature Mater. **7**, 391 (2008).
[5] J. Tao, D. Niebieskikwiat, M. Varela, W. Luo, M. A. Schofield, Y. Zhu, M. B. Salamon, J. M. Zuo, S. T. Pantelides, and S. J. Pennycook, Phys. Rev. Lett. **103**, 097202 (2009).
[6] A. S. McLeod, E. van Heumen, J. G. Ramirez, S. Wang, T. Saerbeck, S. Guenon, M. Goldflam, L. Anderegg, P. Kelly, A. Mueller, M. K. Liu, Ivan K. Schuller, and D. N. Basov, Nature Phys. **13**, 80 (2017).
[7] S. Kumar, J. P. Strachan, M. D. Pickett, A. M. Bratkovsky, Y. Nishi, and R. Stanley Williams, Adv. Mater. **15**, 7505 (2014).
[8] J. Laverock, S. Kittiwatanakul, A. A. Zakharov, Y. R. Niu, B. Chen, S. A. Wolf, J. W. Lu, and K. E. Smith. Phys. Rev. Lett. **113**, 216402 (2014).
[9] M. Imada, A. Fujimori, and Y. Tokura, Rev. Mod. Phys. **70**, 1039 (1998).
[10] A. Asamitsu, Y. Tomioka, H. Kuwahara, and Y. Tokura, Nature **388**, 50 (1997).
[11] D. B. McWhan and J. P. Remeika, Phys. Rev. B **2**, 3734 (1970).
[12] D. Fausti, R. Tobey, N. Dean, S. Kaiser, A. Dienst, M. Hoffmann, S. Pyon, T. Takayama, H. Takagi, and A. Cavalleri, Science **331**, 189 (2011).
[13] K. Kim, A. Pashkin, H. Schafer, M. Beyer, M. Porer, T. Wolf, C. Bernhard, J. Demsar, R. Huber, and A. Leitenstorfer, Nature Mater. **11**, 497 (2012).
[14] D. Y. Lei, K. Appavoo, F. Ligmajer, Y. Sonnefraud, R. F. Haglund, and S. A. Maier, ACS Photonics **2**, 1306 (2015).
[15] V. Kiryukhin, D. Casa, J. P. Hill, B. Keimer, A. Vigliante, Y. Tomioka, and Y. Tokura, Nature **386**, 813 (1997).
[16] K. Miyano, T. Tanaka, Y. Tomioka, and Y. Tokura, Phys. Rev. Lett. **78**, 4257 (1997).
[17] N. Takubo, Y. Ogimoto, M. Nakamura, H. Tamaru, M. Izumi, and K. Miyano, Phys. Rev. Lett. **95**, 017404 (2005).
[18] Y. Okimoto, Y. Ogimoto, M. Matsubara, Y. Tomioka, T. Kageyama, T. Hasegawa, H. Koinuma, M. Kawasaki, and Y. Tokura, Appl. Phys. Lett. **80**, 1031 (2002).
[19] M. Fiebig, K. Miyano, Y. Tomioka, and Y. Tokura, Science **280**, 1925 (1998).
[20] I. I. Smolyaninov, V. N. Smolyaninova, C. C. Davis, B. G. Kim, S. W. Cheong, and R. L. Greene, Phys. Rev. Lett. **87**, 127204 (2001).
[21] J. Zhang, X. Tan, M. Liu, S. W. Teitelbaum, K. W. Post, F. Jin, K. A. Nelson, D. N. Basov, W. Wu, and R. D. Averitt, Nature Mater. **15**, 956 (2016).
[22] P. Beaud, A. Caviezel, S. O. Mariager, L. Rettig, G. Ingold, C. Dornes, S. W. Huang, J. A. Johnson, M. Radovic, T. Huber, T. Kubacka, A. Ferrer, H. T. Lemke, M. Chollet, D. Zhu, J. M. Glownia, M. Sikorski, A. Robert, H. Wadati, M. Nakamura, M. Kawasaki, Y. Tokura, S. L. Johnson, and U. Staub, Nature Mater. **13**, 923 (2014).
[23] T. Li, A. Patz, L. Mouchliadis, J. Yan, T. A. Lograsso, I. E. Perakis, and J. Wang Nature **496**, 69 (2013).
[24] D. Polli, M. Rini, S. Wall, R. W. Schoenlein, Y. Tomioka, Y. Tokura, G. Cerullo, and A. Cavalleri, Nature Mater. **6**, 643 (2007).
[25] J. X. Ma, D. T. Gillaspie, E. W. Plummer, and J. Shen, Phys. Rev. Lett. **95**, 237210 (2005).
[26] H. Ichikawa, S. Nozawa, T. Sato, A. Tomita, K. Ichiyanagi, M. Chollet, L. Guerin, N. Dean, A. Cavalleri, S. Adachi, T. Arima, H. Sawa, Y. Ogimoto, M. Nakamura, R. Tamaki, K. Miyano, and S. Koshihara, Nature Mater. **10**, 101 (2011).
[27] V. R. Morrison, R. P. Chatelain, K. L. Tiwari, A. Hendaoui, A. Bruhacs, M. Chaker, and B. J. Siwick, Science **346**, 445 (2014).
[28] D. N. Basov, R. D. Averitt, D. van der Marel, M. Dressel, and K. Haule, Rev. Mod. Phys. **83**, 471 (2011).
[29] M. Uehara, S. Mori, C. H. Chen, and S. W. Cheong, Nature **399**, 560 (1999).
[30] K. H. Ahn, T. Lookman, and A. R. Bishop, Nature **428**, 401 (2004).
[31] C. Milward, M. J. Calderón, and P. B. Littlewood, Na-

ture **433**, 607 (2005).
[32] L. Zhang, C. Israel, A. Biswas, R. L. Greene, and A. L. de Lozanne, Science **298**, 805 (2002).
[33] W. Wu, C. Israel, N. Hur, S. Park, S. W. Cheong, and A. D. Lozanne, Nature Mater. **5**, 881 (2006).
[34] Du, K. Zhang, S. Dong, W. Wei, J. Shao, J. Niu, J. Chen, Y. Zhu, H. Lin, X.Yin, S. H. Liou, L. Yin, and J. Shen, Nature Commun. **6**, 6179 (2015).
[35] See Supplementary Material in URL ..... (to be provided), which includes Refs. [36–41].
[36] L. Néel, Ann.Geophys **5**, 99 (1949).
[37] B. D. Cullity, *Introduction to magnetic materials*, Addison-Wesley Pub. Co. (1972).
[38] H. Liu, L. Lin, Y. Yu, H. Lin, Y. Zhu, T. Miao, Y. Bai, Q. Shi, P. Cai, Y. Kou, F. Lan, W. Wang, X. Zhou, S. Dong, L. Yin and J. Shen, Phys. Rev. B **96**, 195154 (2017).
[39] D. Rugar, H. J. Mamin, P. H. Guethner, S. E. Lambert, J. E. Stern, I. R. Mcfadyen, and T. Yogi, J. Appl. Phys. **68**, 1169 (1990).
[40] T. E. Schäffer, M. Radmacher, and R. Proksch, J. Appl. Phys. **94**, 6525 (2003).
[41] H. Zhou, L. Wang, Y. Hou, Z. Huang, Q. Lu, and W. Wu, Nature. Commun. **6**, 8980 (2015).
[42] N. Takubo, I. Onishi, K. Takubo, T. Mizokawa, and K. Miyano, Phys. Rev. Lett. **101**, 177403 (2008).
[43] The two curves were measured in two independent thermal cycles to reset the samples' ρ to the same value before photoexcitation.
[44] See also Fig. S1 [35] for 105 and 190 K.
[45] LPCMO thin films with an in-plane easy axis, see K. Zhang, K. Du, H. Liu, X. Zhang, F. Lan, H. Lin, W. Wei, Y. Zhu, Y. Kou, J. Shao, J. Niu, W. Wang, R. Wu, L. Yin, E. W. Plummer, and J. Shen, PNAS **112**, 9558 (2015).
[46] C. P. Bean and J. D. Livingston, J. Appl. Phys. **30**, S120 (1959).
[47] J. Shen, R. Skomski, M. Klaua, H. Jenniches, S. S. Manoharan, and J. Kirschner, Phys. Rev. B **56**, 2340 (1997).
[48] J. Shen, J. P. Pierce, E. W. Plummer, and J. Kirschner, J. Phys.: Condens. Matter **15**, R1 (2003).
[49] Z. Q. Qiu and S. D. Bader, J. Magn. Magn. Mater. **200**, 664 (1999).
[50] J. Burgy, M. Mayr, V. Martin-Mayor, A. Moreo, and E. Dagotto, Phys. Rev. Lett. **87**, 277202 (2001).
[51] S. Dong, H. Zhu, X. Wu, and J. M. Liu, Appl. Phys. Lett. **86**, 022501 (2005).
[52] K. Lai, M. Nakamura, W. Kundhikanjana, M. Kawasaki, Y. Tokura, M. A. Kelly, and Z. Shen, Science **329**, 190-193 (2010).
[53] A. Moreo, M. Mayr, A. Feiguin, S. Yunoki, and E. Dagotto, Phys. Rev. Lett. **84**, 5568 (2000).
[54] E. Dagotto, T. Hotta, and A. Moreo, Phys. Rep. **344**, 1 (2001).
[55] Y. Zhu, K. Du, J. Niu, L. Lin, W. Wei, H. Liu, H. Lin, K. Zhang, T. Yang, Y. Kou, J. Shao, X. Gao, X. Xu, X. Wu, S. Dong, L. Yin, and J. Shen, Nat. Commun. **7**, 11260 (2016).
[56] E. Dagotto, New J. Phys. **7**, 67 (2005). See also H. Aliaga, D. Magnoux, A. Moreo, D. Poilblanc, S. Yunoki, and E. Dagotto, Phys. Rev. B **68**104405 (2003) and J. Burgy, E. Dagotto, and M. Mayr, Phys. Rev. B **67**, 014410 (2003).
[57] Y. Tokura, H. Kuwahara, Y. Moritomo, Y. Tomioka, and A. Asamitsu, Phys. Rev. Lett. **76**, 3184 (1996).
[58] L. Stojchevska, I. Vaskivskyi, T. Mertelj, P. Kusar, D. Svetin, S. Brazovskii, D. Mihailovic, Science, **344**, 177 (2014).
[59] C. S. Nelson, M. v. Zimmermann, Y. J. Kim, J. P. Hill, Doon Gibbs, V. Kiryukhin, T. Y. Koo, S.-W. Cheong, D. Casa, B. Keimer, Y. Tomioka, Y. Tokura, T. Gog, and C. T. Venkataraman, Phys. Rev. B **64**, 174405 (2001)
[60] E. Dagotto, Science, **309**, 257 (2005).